6456 *Inorg. Chem.* **1995,** *34,* 6456–6462

Trivalent Transition Metal Complexes [M^{III}(L-3H)] (M = Fe, Co) of the Triply Deprotonated Hexadentate Ligand 1,4,7-Tris(*o*-aminobenzyl)-1,4,7-triazacyclononane (L). Crystal Structure of [Mn^{IV}(L-3H)]BPh_4

Oliver Schlager,[1a] Karl Wieghardt,*,[1a] and Bernhard Nuber[1b]

Max-Planck-Institut für Strahlenchemie, D-45470 Mülheim, Germany, and Anorganisch-Chemisches Institut der Universität, D-69120 Heidelberg, Germany

Received June 7, 1995®

Air oxidation of [Fe^{II}L]$(ClO_4)_2$ and [Co^{II}L]$(ClO_4)_2$ in acetonitrile in the presence of NEt_3 affords deep blue and red microcrystals of [Fe^{III}(L-3H)] and [Co^{III}(L-3H)], respectively (L = 1,4,7-tris(*o*-aminobenzyl)-1,4,7-triazacyclononane, and L-3H is its triply deprotonated trianion). The reaction of L with "manganese(III) acetate" in ethanol in the presence of air yields a deep blue solution from which, upon addition of Na[BPh_4], dark blue crystals of [Mn^{IV}(L-3H)]BPh_4 were obtained. The same material was obtained from air oxidation of an CH_3CN solution of [Mn^{II}L]$(ClO_4)_2$ to which NEt_3 and $NaBPh_4$ had been added. The crystal structure of the manganese(IV) complex has been determined by single-crystal X-ray crystallography. [Mn^{IV}(L-3H)]BPh_4 crystallizes in the orthorhombic space group *Pbca* with $Z = 8$, $a = 19.700(9)$ Å, $b = 20.255(7)$ Å, and $c = 21.092(5)$ Å. The manganese(IV) ion is in a distorted octahedral environment of three facially coordinated tertiary nitrogen donor atoms and three anilido nitrogen donors. The cation possesses idealized C_3 symmetry.

Introduction

In the previous two papers[2,3] we have investigated the coordination chemistry of the hexadentate ligand 1,4,7-tris(*o*-aminobenzyl)-1,4,7-triazacyclononane (L) with divalent transition metal ions. We have shown that in a complex with a d^n electronic configuration which has no or only a small preference for octahedral over trigonal prismatic coordination (d^5 hs, d^6 hs, d^7 hs, d^{10}), a distorted trigonal prismatic MN_6 polyhedron prevails due to the steric requirements of the ligand. Thus the complexes [M^{II}L]$(ClO_4)_2$ (M = Zn, Mn, Fe, Co) were found to be isostructural (Figure 1).

The dications possess C_1 symmetry in the solid state where two of the three six-membered pendent arm chelates adopt a boat and the third a twist-boat conformation. In contrast, in [NiL]$(ClO_4)_2$ the dication has a distorted octahedral NiN_6 polyhedron and all three six-membered chelates adopt a boat conformation leading to C_3 symmetry. This has been attributed to the electronic preference of a d^8 electronic configuration for an octahedral rather than trigonal prismatic ligand environment.

During the preparation of [Mn^{II}L]$(ClO_4)_2$, [Fe^{II}L]$(ClO_4)_2$, and [Co^{II}L]$(ClO_4)_2$,[3] we found that these three complexes are air-sensitive in solution. Here we report the nature of the oxidation products which were found to contain the coordinated triply deprotonated form of L, namely the tris(anilide) (L-3H), and the corresponding tetravalent or trivalent transition metal ion. We also report here the crystal structure of [Mn^{IV}(L-3H)]BPh_4.

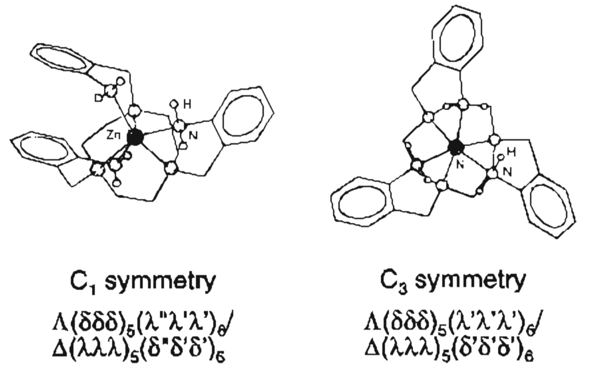

Figure 1. Structures of the C_1-symmetric dication in crystals of [ZnL]$(ClO_4)_2$ and of the C_3-symmetric dication in crystals of [NiL]$(ClO_4)(BPh_4)((CH_3)_2CO)_2$. Λ, Δ denote the configuration of the MN_6 polyhedron, λ, δ the conformation of the five-membered chelate rings of the 1,4,7-triazacyclononane backbone, and λ′, δ′ the boat and λ″, δ″ the twist-boat conformation of the six-membered pendant arm chelate rings.

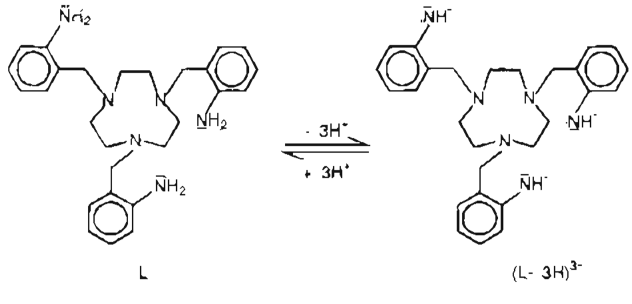

Experimental Section

The ligand 1,4,7-tris(*o*-aminobenzyl)-1,4,7-triazacyclononane (L) was prepared as described previously.[2]

Preparation of Complexes. [Fe^{III}(L-3H)]. To a solution of [Fe^{II}L]$(ClO_4)_2$[3] (0.20 g; 0.29 mmol) in acetonitrile (20 mL) were added three drops of triethylamine in the presence of air at ambient temperature. A color change to deep blue was observed. Within 2 d of standing in an open vessel at 20 °C, deep blue crystals precipitated, which were collected by filtration, washed with ethanol and ether, and air-dried. Yield: 0.13 g (90%). Anal. Calcd for $C_{27}H_{33}N_6Fe$: C, 64.0; H, 6.6; N, 16.6; Fe, 11.0. Found: C, 63.6; H, 6.4; N, 16.8; Fe, 10.7. Mass spectroscopy: molecular ion peak $m/z = 497$ (100%) (calcd 497.4).

® Abstract published in *Advance ACS Abstracts,* November 15, 1995.

(1) (a) Max-Planck-Institut für Strahlenchemie. (b) Universität Heidelberg.
(2) Schlager, O.; Wieghardt, K.; Grondey, H.; Rufińska, A.; Nuber, B. *Inorg. Chem.* **1995**, *34*, 6440.
(3) Schlager, O.; Wieghardt, K.; Nuber, B. *Inorg. Chem.* **1995**, *34*, 6449.

0020-1669/95/1334-6456$09.00/0

Table 1. Crystallographic Data for $[Mn^{IV}(L\text{-}3H)]BPh_4$

empirical formula	$C_{51}H_{53}N_6BMn$
fw	815.8
space group	*Pbca* (No. 61)
a, Å	19.700(9)
b, Å	20.255(7)
c, Å	21.092(5)
Z	8
ρ(calcd), g cm^{-3}	1.29
temp, °C	22
radiation (λ, Å)	Mo Kα (0.710 73)
abs coeff, mm^{-1}	0.34
min/max transm coeff	0.96/1.00
R^a	0.068
$R_w{}^b$	0.058

$^a R = \sum(|F_o| - |F_c|)/\sum|F_o|$. $^b R_w = \{\sum w(|F_o| - |F_c|)^2/\sum w(|F_o|)^2\}^{1/2}$.

$[Co^{III}(L\text{-}3H)]$. This complex was prepared as described above for [Fe(L-3H)] by using $[CoL](ClO_4)_2$[3] as starting material. Deep-red microcrystals were obtained. Yield: 0.12 g (90%). Anal. Calcd for $C_{27}H_{33}N_6Co$: C, 62.5; H, 6.8; N, 16.2; Co, 11.4. Found: C, 62.9; H, 7.1; N, 16.4; Co, 10.7. Mass spectroscopy: molecular ion peak *m*/*z* = 500 (18%) (calcd 500.5).

$[Mn^{IV}(L\text{-}3H)]BPH_4$. To a solution of the ligand L (0.22 g; 0.5 mmol) in ethanol (25 mL) was added "manganese(III) acetate" (0.14 g). Within a few minutes of stirring at ambient temperature in the presence of air, a color change from yellow to deep blue was observed. After continuous stirring for 1 h and filtration, a solution of sodium tetraphenylborate (0.17 g; 0.5 mmol) in ethanol (10 mL) was added, which initiated the precipitation of dark-blue microcrystals. These were collected by filtration and washed with ethanol and ether. Yield: 0.21 g (52%). Anal. Calcd for $C_{51}H_{53}N_6BMn$: C, 75.1; H, 6.6; N, 10.3. Found: C, 71.9; H, 6.2; N, 9.8.

Single crystals of this compound suitable for X-ray crystallography were obtained by synthesizing the complex as above but in acetone solution (25 mL) and with the addition of only 0.08 g of $Na[BPh_4]$. Slow evaporation of the solvent at room temperature produced black-blue single crystals.

The above complex was also prepared by air oxidation of an acetonitrile solution of $[Mn^{II}L](ClO_4)_2$ to which a few drops of NEt_3 had been added. The same reaction conditions as described above for [Fe(L-3H)] were used, but an equimolar amount of $Na[BPh_4]$ was added to the deep blue solution in order to precipitate $[Mn(L\text{-}3H)]BPh_4$.

Crystal Structure Determination. Intensities and lattice parameters of a deep blue, brick-shaped crystal of $[Mn(L\text{-}3H)]BPh_4$ were measured on a Syntex R3 diffractometer at ambient temperature by using monochromated Mo Kα radiation. Crystal parameters and details of the data collection and refinement are summarized in Table 1 (for full details see the Supporting Information). An empirical absorption correction (ψ scans) was carried out. The structure was solved by direct and difference Fourier methods. The Siemens program package SHELXTL-PLUS was used.[4] The function minimized during full-matrix least-squares refinement was $\sum w(|F_o| - |F_c|)^2$ where $w^{-1} = \sigma^2(F)$. Neutral-atom scattering factors and anomalous-dispersion corrections for non-hydrogen atoms were taken from ref 5. The positions of the methylene and phenyl hydrogen atoms were placed at calculated positions with isotropic thermal parameters; anilide hydrogen atom positions were located in the difference Fourier map and were refined with a fixed isotropic thermal parameter ($U = 0.080$ Å^2). Table 2 gives atom coordinates for $[Mn(L\text{-}3H)]BPh_4$.

Physical Measurements. Infrared spectra were recorded in the 4000–400 cm^{-1} range as KBr disks on a Perkin-Elmer FT IR 1720 X spectrometer. UV–vis spectra were measured on a Perkin-Elmer Lambda 9 spectrophotometer. Magnetic susceptibility data were obtained by using the Faraday method. Data were corrected for underlying diamagnetism by use of tabulated Pascal constants. Cyclic voltammograms were recorded on PAR equipment consisting of a Model 173/179 potentiostat/galvanostat with a Model 175 universal programmer.

Table 2. Atomic Coordinates ($\times 10^4$) and Equivalent Isotropic Displacement Parameters ($\times 10^3$) for $[C_{27}H_{33}N_6Mn](BC_{24}H_{20})$

atom	*x*	*y*	*z*	*U*(eq)^a
Mn1	2585(1)	2979(1)	−234(1)	34(1)
N1	2217(2)	3935(2)	−66(2)	42(2)
N2	1766(2)	2940(2)	−869(2)	40(1)
N3	3078(2)	3438(2)	−997(2)	41(2)
N4	2856(2)	2122(2)	−482(2)	39(1)
N5	3352(2)	3110(2)	276(2)	40(1)
N6	2066(2)	2650(2)	438(2)	39(1)
C1	1556(3)	4042(3)	−401(3)	51(2)
C2	1245(3)	3393(3)	−600(3)	52(2)
C3	1989(3)	3163(3)	−1527(2)	49(2)
C4	2760(3)	3144(3)	−1579(2)	47(2)
C5	2971(3)	4168(2)	−981(3)	49(2)
C6	2750(3)	4391(2)	−322(2)	49(2)
C7	2153(3)	4073(3)	631(2)	45(2)
C8	1460(3)	2264(3)	−895(3)	51(2)
C9	3818(3)	3274(3)	−1001(2)	46(2)
C10	1673(3)	3637(3)	989(2)	39(2)
C11	1272(3)	3911(3)	1461(2)	47(2)
C12	890(3)	3518(3)	1864(3)	55(2)
C13	913(3)	2840(3)	1796(3)	60(2)
C14	1297(3)	2557(3)	1326(2)	47(2)
C15	1685(2)	2946(3)	908(2)	38(2)
C16	1922(3)	1742(3)	−1141(2)	44(2)
C17	1694(3)	1293(3)	−1591(3)	54(2)
C18	2082(4)	777(3)	−1797(3)	68(3)
C19	2716(3)	694(3)	−1545(3)	56(2)
C20	2971(3)	1127(2)	−1097(2)	45(2)
C21	2590(3)	1668(2)	−899(2)	38(2)
C22	4197(3)	3553(3)	−443(3)	47(2)
C23	4808(3)	3883(3)	−525(3)	61(2)
C24	5191(3)	4087(3)	−16(3)	75(3)
C25	4962(3)	3967(3)	595(3)	70(3)
C26	4357(3)	3643(3)	690(3)	52(2)
C27	3959(3)	3428(2)	174(3)	40(2)
B1	3831(3)	1168(3)	1467(3)	34(2)
C31	4926(2)	395(2)	1674(1)	52(2)
C32	5332	−5	2056	66(3)
C33	5155	−113	2688	62(3)
C34	4573	181	2938	58(2)
C35	4167	581	2557	48(2)
C36	4344	688	1924	36(2)
C37	4241(2)	705(1)	361(2)	48(2)
C38	4537	761	−238	59(2)
C39	4774	1372	−448	66(3)
C40	4716	1927	−60	60(2)
C41	4421	1871	539	47(2)
C42	4183	1260	749	36(2)
C43	4279(1)	2191(2)	2141(2)	59(2)
C44	4212	2816	2412	70(3)
C45	3599	3156	2364	57(2)
C46	3052	2870	2045	50(2)
C47	3119	2245	1774	40(2)
C48	3732	1905	1822	37(2)
C49	2704(2)	988(2)	801(1)	43(2)
C50	2032	788	718	52(2)
C51	1702	437	1196	65(3)
C52	2044	285	1757	78(3)
C53	2716	485	1839	57(2)
C54	3046	836	1361	36(2)

^{a} Equivalent isotropic *U* defined as one-third of the trace of the orthogonalized $\mathbf{U}_{ij}$ tensor.

Results

Synthesis and Spectroscopic Characterization of Complexes. [Fe(L-3H)]. When a yellow solution of $[Fe^{II}L](ClO_4)_2$ in acetonitrile or acetone to which a few drops of triethylamine had been added was exposed to air, a color change to deep blue

---

(4) Full-matrix least-squares structure refinement program package SHELXTL-PLUS: G. M. Sheldrick, Universität Göttingen.

(5) *International Tables for Crystallography*; Kynoch: Birmingham, England, 1974; Vol. IV, pp 99, 149.

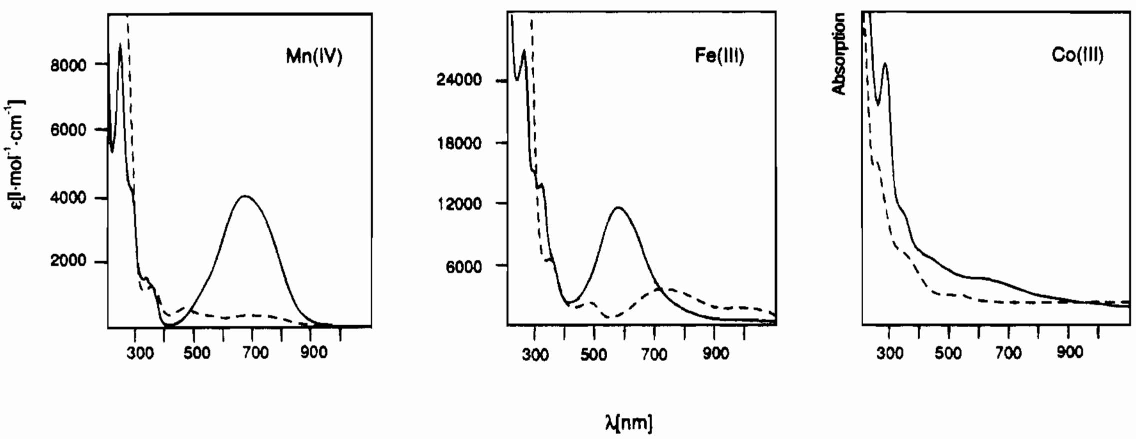

Figure 2. Electronic spectra of [Co^{III}(L-3H)], [Fe^{III}(L-3H)], and [Mn^{IV}(L-3H)]BPh$_4$ in acetonitrile (solid lines) and of their triply protonated forms [M^{III}L]$^{3+}$ and [Mn^{IV}L]$^{4+}$ in CH$_3$CN/HClO$_4$ (broken lines).

was observed within a few seconds. From such a solution blue-black crystals of [Fe^{III}(L-3H)] precipitated within 2 d. The material was soluble in acetonitrile to which a few drops of concentrated HClO$_4$ had been added with change of color to pale green. Figure 2 shows the electronic spectra of [Fe^{III}(L-3H)] and its presumably triply protonated, pale green form [Fe^{III}L]$^{3+}$. The dominant feature of the spectrum of [Fe(L-3H)] is a very intense charge transfer band at 587 nm (anilide → iron(III)) with a molar absorption coefficient of 8.7 × 10^3 L mol^{-1} cm^{-1} which upon protonation of the coordinated R−NH groups disappears by forming three coordinated R−NH$_2$ ligands. This protonation−deprotonation process is completely reversible, eq 1, and resembles the behavior of orange [Fe^{III}(tacn)$_2$]$^{3+}$

$$[\mathrm{Fe^{III}(L\text{-}3H)}] + 3\mathrm{H}^+ \rightleftarrows [\mathrm{Fe^{III}L}]^{3+} \qquad (1)$$

(tacn = 1,4,7-triazacyclononane), which in basic solution forms reversibly the deep blue amido species [Fe^{III}(tacn)(tacn-H)]$^{2+}$.[6] We have as yet not been able to isolate a crystalline salt of the protonated form.

In the infrared spectrum of [Fe^{III}(L-3H)], one sharp band at 3313 cm^{-1} is indicative of three equivalent anilido groups (ν(N−H)); the ν(C−N) stretching mode of the anilido groups is observed at 1306 cm^{-1}. From magnetic susceptibility measurements in the range 80−298 K, a temperature-independent magnetic moment of 5.9 μ_B clearly indicates a high-spin d^5 electronic configuration of the iron(III) center in [Fe(L-3H)]. Thus the three strong π-donor anilido groups effectively generate a weak ligand field. In contrast, the complexes containing pure σ-donor ligands [Fe^{III}(tacn)$_2$]$^{3+}$ [6] (tacn = 1,4,7-triazacyclononane) and [Fe(dtne)]Br$_3$·4H$_2$O[7] are low spin (t$^5_{2g}$) (dtne = 1,2-bis(1,4,7-triaza-1-cyclononyl)ethane). A weak ligand field is also generated by three thiophenolate groups of coordinated 1,4,7-tris(4-*tert*-butyl-2-mercaptobenzyl)-1,4,7-triazacyclononane (L′) in [Fe^{III}L′], which demonstrates the π-donor capability of RS$^-$ groups.[8]

The cyclic voltammogram of [Fe(L-3H)] in dry dimethylformamide containing 0.10 M tetra-*n*-butylammonium hexafluorophosphate at a glassy carbon working electrode shows a reversible one-electron reduction wave at −1.32 V vs Ag/AgCl (saturated LiClO$_4$, C$_2$H$_5$OH), which shows the stabilization of the trivalent oxidation state by three anilido groups. The tris(phenolato) complex [Fe^{III}(tatp)]^0 (tatpH$_3$ = 1,4,7-tris-(3-*tert*-butyl-2-hydroxybenzyl)-1,4,7-triazacyclononane) is also very stable as compared to its divalent counterpart [Fe(tatp)]$^-$ ($E_{1/2}$ = −1.33 V vs Ag/AgCl)[10] and contrasts the redox potentials of 0.255 and −0.025 V vs Ag/AgCl for [Fe(tacn)$_2$$^{3+/2+}$][9] and [Fe(dtne)]$^{3+/2+}$,[7] respectively.

Table 3. Electronic Spectral and Magnetic Properties of the Complexes

complex	λ_{max}, nm (ϵ, L mol^{-1} cm^{-1})^a	μ_{eff}(298 K), μ_B
[Fe(L-3H)]	264 (1.4 × 10^4), 327 (8.2 × 10^3), 587 (8.7 × 10^3)^b	5.9
[Co(L-3H)]	282, ~350, 440, 600^c	*d*
[Mn(L-3H)]-BPh$_4$	240 (sh), 293 (8.0 × 10^3), 350 (sh), 677 (4.0 × 10^3)	4.0

^{a} Solvent: CH$_3$CN. ^{b} Solvent: CH$_2$Cl$_2$. ^{c} Reflectance spectrum. ^{d} Temperature-independent paramagnetism of χ_M = 480 × 10^{-6} emu in the range 80−298 K.

The structure of [Fe(L-3H)] is assumed to be identical with that of [Co(L-3H)] and [Mn^{IV}(L-3H)]$^+$ containing three six-membered anilido chelate rings (C_3 symmetry).

[Co^{III}(L-3H)]. Air oxidation at ambient temperature of [Co^{II}L](ClO$_4$)$_2$ dissolved in acetonitrile to which a few drops of triethylamine had been added yielded deep-red, nearly black microcrystals of [Co^{III}(L-3H)] within a few hours. In the infrared spectrum, one sharp ν(N−H) stretching frequency at 3347 cm^{-1} indicates the presence of three equivalent coordinated anilido groups; the ν(C−N) stretch of the anilido groups is observed at 1333 cm^{-1}.

[Co(L-3H)] is very insoluble in all common polar and unpolar solvents. Therefore, we have only been able to obtain a reflectance electronic spectrum (Table 3). The band at 560 nm may be assigned to a d−d transition (^{1}A$_{1g}$ → ^{1}T$_{1g}$ in O_h symmetry). In an acetonitrile/HClO$_4$ mixture [Co(L-3H)] dissolves in small amounts with protonation of the three anilido groups, which is completely analogous to the behavior of [Fe^{III}(L-3H)] described in eq 1. The protonation reaction is also reversible. Addition of triethylamine to such a solution regenerates [Co(L-3H)].

Magnetic susceptibility measurements of a powdered sample of [Co(L-3H)] in the temperature range 80−298 K obtained by the Faraday method reveal a temperature-independent paramagnetism, χ_{TIP}, of 480 × 10^{-6} emu after correcting the data for underlying diamagnetism (−158 × 10^{-6} emu). We feel that

---

(6) Pohl, K.; Wieghardt, K.; Kaim, W.; Steenken, S. *Inorg. Chem.* **1988**, *27*, 440.

(7) Geilenkirchen, A.; Wieghardt, K.; Nuber, B.; Weiss, J. *Z. Naturforsch.* **1989**, *44B*, 1333.

(8) Beissel, T.; Bürger, K. S.; Voigt, G.; Wieghardt, K. *Inorg. Chem.* **1993**, *32*, 124.

(9) Wieghardt, K.; Schmidt, W.; Herrmann, W.; Küppers, H.-J. *Inorg. Chem.* **1983**, *22*, 2953.

(10) Auerbach, U.; Eckert, U.; Wieghardt, K.; Nuber, B.; Weiss, J. *Inorg. Chem.* **1990**, *29*, 938.

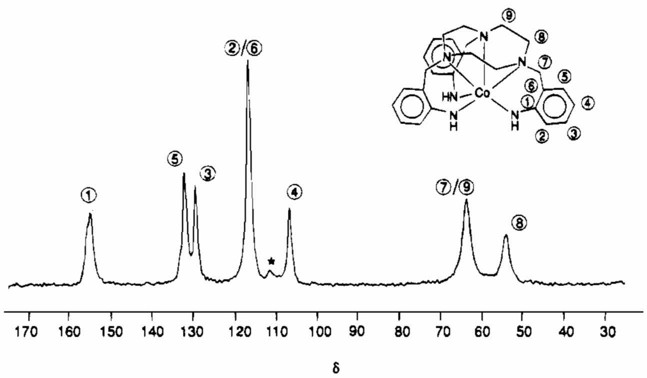

Figure 3. Solid state magic angle spinning ^{13}C NMR spectrum of [Co(L-3H)] and assignment of resonances. The asterisk denotes an unknown impurity.

this is a genuine property of [Co(L-3H)] and is not caused by a small Co(II) impurity.[11]

Although it has not been possible to obtain solution ^1H and ^{13}C NMR spectra, we have obtained a solid state magic angle spinning ^{13}C NMR spectrum of [Co(L-3H)], which is displayed in Figure 3. For a C_3-symmetric species, nine carbon resonances are expected of which seven are experimentally observed. The spectrum clearly differs from the corresponding spectrum reported for the C_1 symmetric species $[ZnL](ClO_4)_2$ (Figure 7 in ref 2). Therefore, we conclude that [Co(L-3H)] has the same C_3-symmetric structure as the cation in $[Mn(L-3H)]BPh_4$ (see below).

$[Mn^{IV}(L-3H)]BPh_4$. From the reaction mixture of $[Mn^{III}_3(\mu_3\text{-}O)(\mu\text{-}CH_3CO_2)_6]CH_3CO_2$ (manganese(III) acetate) and the ligand L (1:3) in ethanol in the presence of air at room temperature a deep-blue solution was obtained within a few seconds. Addition of an equimolar amount of sodium tetraphenylborate initiated the precipitation of blue-black crystals of $[Mn^{IV}(L-3H)]BPh_4$ in 52% yield. When the same reaction was carried out under anaerobic conditions, the same product was generated but in only half the yield. This implies that a disproportionation reaction occurs under these experimental conditions, eq 2. This

$$2L + 2Mn(III) \rightarrow [Mn^{IV}(L-3H)]^+ + [Mn^{II}L]^{2+} \qquad (2)$$

was verified by UV-vis spectroscopy. $[Mn^{IV}(L-3H)]^+$ displays a very intense absorption maximum in the visible region at 677 nm ($\epsilon = 1.8 \times 10^3$ L mol^{-1} cm^{-1}) whereas $[Mn^{II}L]^{2+}$ is colorless. The reaction in the presence of air yields quantitatively $[Mn(L-3H)]^+$, but under anaerobic conditions only 50% is formed. The same blue solution was obtained when an acetonitrile solution of $[Mn^{II}L](ClO_4)_2$[3] to which a few drops of NEt_3 had been added was exposed to air at ambient temperature. Blue $[Mn(L-3H)]BPh_4$ precipitated upon addition of $Na[BPh_4]$.

$[Mn(L-3H)]BPh_4$ readily dissolves in acetonitrile, and addition of concentrated $HClO_4$ induces a color change to orange-brown (Figure 2). The intense anilide-to-manganese(IV) charge transfer band is now absent, indicating that protonation at the three coordinated anilido groups has occurred.

From magnetic susceptibility data a temperature-independent magnetic moment of 4.0 μ_B (80–298 K) was found in agreement with a d^3 electronic configuration of manganese(IV). Figure 4 shows the X-band ESR spectrum of a solid sample of $[Mn(L-3H)]BPh_4$ at 10 K. A nearly axial signal with $g_\perp = 3.55$ and $g_\parallel = 1.95$ is observed. ^{55}Mn hyperfine interaction is hinted at the $g_\parallel$ signal. Since the signal at ~4.0 is the more intense, it is concluded that $[Mn(L-3H)]^+$ is a species with large zero-field splitting ($2D \gg h\nu \sim 0.3$ cm^{-1}). Similar ESR spectra have been reported for $[Mn^{IV}(HB(3,5\text{-}Me_2pz)_3)_2](ClO_4)_2$[12] and $[Mn\text{-}TPP(NCO)_2]$,[13] both of which contain a distorted octahedral $Mn^{IV}N_6$ polyhedron. Pecoraro et al.[14] have reported a spectrum for $[Mn^{IV}(saladhp)_2]$ (saladhp = 1,3-dihydroxy-2-methyl(2-salicylideneaminato)propane) where both signals show hyperfine splitting, and Chakravorty et al. have reported a spectrum with hyperfine splitting at the $g \sim 2.0$ signal only for $Mn(als)_2$ where als represents *N*-(2-carboxyethyl)salicylideneaminate.[15]

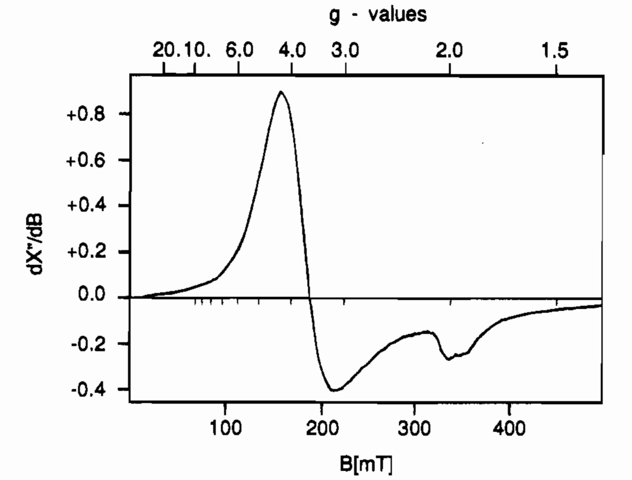

Figure 4. X-band ESR spectrum of solid $[Mn(L-3H)]BPh_4$ at 10 K (9.4317 GHz microwave frequency).

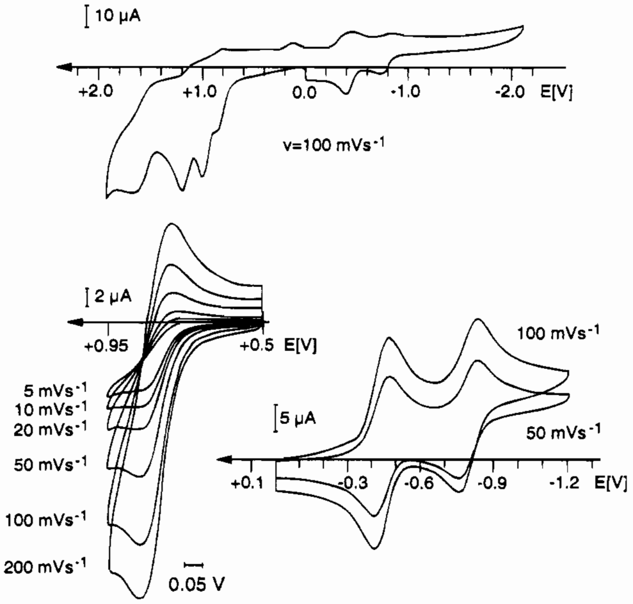

Figure 5. Cyclic voltammogram of $[Mn(L-3H)]BPh_4$ in acetonitrile at a glassy carbon working electrode and a Ag/AgCl (saturated $LiClO_4$, ethanol) reference electrode (conditions: 0.10 M $[TBA]PF_6$ supporting electrolyte; $[Mn^{IV}] = 4.4 \times 10^{-4}$ M: top, scan range +2.0 to −2.1 V vs Ag/AgCl; bottom left, scan range +0.50 to +0.95 V vs Ag/AgCl; bottom right, scan range +0.10 to −1.20 V vs Ag/AgCl).

Figure 5 shows the cyclic voltammogram of $[Mn(L-3H)]BPh_4$ (4×10^{-4} M) in acetonitrile containing 0.10 M $[TBA]PF_6$ as supporting electrolyte at a glassy carbon electrode in the

---

[11] Figgis, B. N.; Lewis, J. *Prog. Inorg. Chem.* **1964**, *6*, 37.

[12] Chan, M. K.; Armstrong, W. H. *Inorg. Chem.* **1989**, *28*, 3779.

[13] Camenzind, M. J.; Hollander, F. J.; Hill, C. L. *Inorg. Chem.* **1983**, *22*, 3776.

[14] Kessissoglou, D. P.; Li, X.; Butler, W. M.; Pecoraro, V. L. *Inorg. Chem.* **1987**, *26*, 2487.

[15] Chandra, S. K.; Basu, P.; Ray, D.; Pal, S.; Chakravorty, A. *Inorg. Chem.* **1990**, *29*, 2423.

Table 4. Comparison of Redox Potentials of the Mn^{IV} Complexes

complex[b]	$E_{1/2}(Mn^{IV}/Mn^{III})$, V[a]	$E_{1/2}(Mn^{III}/Mn^{II})$, V[a]	ref
$[Mn(HB(3,5\text{-}Me_2pz)_3)_2]$-$(ClO_4)_2$	+1.39	+0.06	12
$[Mn(big)_3]O_2CCH_3\cdot 2H_2O$	−0.69 (irr)		18
$[Mn(sal)_2(bpy)\}$	−046 (irr)		20
$[MnL^1]\cdot 4H_2O$	−0.23		21
$K_2[Mn(L^2)_2]\cdot 3.5H_2O$	−0.85		16
$[Mn(L\text{-}3H)]BPh_4$	−0.44	−0.815	this work
$[MnL^3]$	+0.05	−0.48	10

[a] Potentials are referenced vs Ag/AgCl (saturated $LiClO_4$, C_2H_5OH). [b] Ligand abbreviations: $\{HB(3,5\text{-}Me_2pz)_3\}^-$ = hydrotris(3,5-dimethylpyrazolyl)borate; big^- = biguanide; sal = salicylate; bpy = 2,2′-bipyridine; L^1 = *N,N*′-bis(ethylsalicylamido)ethylenediamine; L^2 = *N*-(2-hydroxyphenyl)salicylamide(3−); L^3 = 1,4,7-tris(3-*tert*-butyl-2-hydroxybenzyl)-1,4,7-triazacyclononane.

potential range +0.10 to −1.3 V vs Ag/AgCl at scan rates of 50 and 100 mV s^{-1}. Two reversible one-electron transfer waves are observed at $E^1{}_{1/2} = -0.44$ V and $E^2{}_{1/2} = -0.815$ V vs Ag/AgCl which are assigned to the Mn^{IV}/Mn^{III} and Mn^{III}/Mn^{II} couples, respectively. When the scanned potential range is expanded to more positive potentials (+2.0 V), a further reversible one-electron oxidation wave at $E^3{}_{1/2} = +0.81$ V vs Ag/AgCl and three irreversible oxidation peaks at $E_{p,ox} = +0.98$, 1.185, 1.65 V vs Ag/AgCl are detected. The irreversible oxidation at +0.98 V is due to oxidation of the tetraphenylborate anion, since addition of sodium tetraphenylborate enhances this signal. The reversible oxidation at $E^3{}_{1/2} = 0.81$ V vs Ag/AgCl may be a metal-centered oxidation of Mn^{IV} to Mn^V. This has been proposed by Okawa et al.[16] for some manganese(IV) complexes containing *N*-(2-hydroxyphenyl)salicylamide ligands. These autors argued that the trianionic form of the ligand with phenolate and amide functionalities stabilizes octahedral manganese(V) and even manganese(VI). This could also apply for three anilido groups in $[Mn^{IV}(L\text{-}3H)]^+$. On the other hand, it is also conceivable that a reversible one-electron oxidation of a coordinated phenolate or anilido function generates a coordinated phenoxy or, analogously, a coordinated $R-\dot{N}H$ radical which is antiferromagnetically coupled to the $t^3{}_{2g}$ electrons at the metal center. This was recently shown to be the case in $[Fe^{III}L']$ complexes where L′ is the trianion tris(3- or 5-*tert*-butyl-2-oxybenzyl)-1,4,7-triazacyclononane.[17] The other two irreversible oxidations almost certainly involve oxidation of the aniline pendant arms (2e processes?).

Table 4 summarizes reported redox potentials for some octahedral Mn^{IV} species. The $E_{1/2}$ values for the Mn^{IV}/Mn^{III} couple span the range +1.39 V vs Ag/AgCl for Armstrong's complex $[Mn^{IV}(HB(3,5\text{-}Me_2pz)_3)_2](ClO_4)_2$[12] to −0.85 V vs Ag/AgCl for Okawa's complex.[16] From these data it clearly follows that alkoxy, phenolate amide, and anilide ligands capable of strong π-donation to the highly oxidized manganese(IV) ion stabilize this oxidation state very effectively[14] whereas Mn^{IV} complexes containing pure σ-donors (or π-acceptors) such as Armstrong's tris(pyrazolyl)borate ligands are strong oxidants.

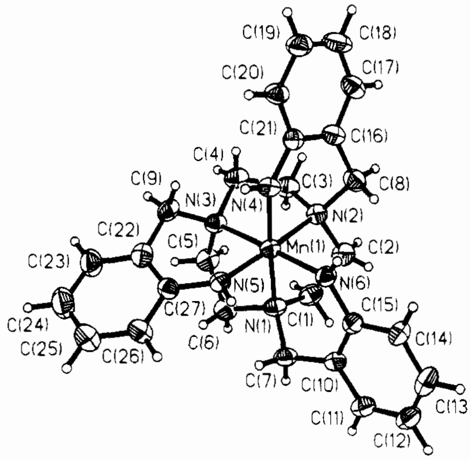

Figure 6. Structure of the monocation in crystals of $[Mn(L\text{-}3H)]BPh_4$.

Table 5. Selected Bond Distances (Å) and Angles (deg) for $[Mn^{IV}(L\text{-}3H)]BPh_4$

Mn1−N1	2.099(4)	Mn1−N4	1.888(4)
Mn1−N2	2.099(4)	Mn1−N5	1.873(4)
Mn1−N3	2.097(4)	Mn1−N6	1.869(4)
N4−C21	1.377(6)	N5−C27	1.376(7)
N6−C15	1.382(7)	N4−H	0.86(5)
N5−H	0.79(5)	N6−H	0.80(5)
N1−Mn1−N2	82.9(2)	N1−Mn1−N2	83.1(2)
N2−Mn1−N3	83.2(2)	N5−Mn1−N6	93.2(2)
N4−Mn1−N6	92.2(2)	N4−Mn1−N5	93.5(2)
Mn1−N4−C21	133.1(3)	Mn1−N5−C27	132.7(4)
Mn1−N6−C15	133.4(3)	Mn1−N4−H	109(4)
Mn1−N5−H	114(4)	C21−N4−H	118(4)
C27−N5−H	112(4)	C15−N6−H	107(4)
Mn1−N6−H	119(4)	N3−Mn1−N6	173.0(2)
N1−Mn1−N4	172.8(2)	N2−Mn1−N5	172.6(2)

Crystal Structure of $[Mn(L\text{-}3H)]BPh_4$. Figure 6 shows the structure of the monocation $[Mn(L\text{-}3H)]^+$ in crystals of $[Mn(L\text{-}3H)]BPh_4$, and Table 5 gives selected bond distances and angles.

The manganese(IV) ion of the cation is in a distorted octahedral environment composed of three facially coordinated amine nitrogen donors of the 1,4,7-triazacyclononane backbone and three anilide nitrogen donor atoms of the three pendant arms of the ligand L. Since the hydrogen atoms of the anilide groups have been located in the difference Fourier map and were successfully refined, it is meaningful to discuss the geometrical details of the coordinated $R-NH^-$ groups. These nitrogen atoms are three-coordinate. The sum of the three bond angles at these nitrogen atoms is very close to 360° (359.2, 359.6, and 359.7°), and hence, these nitrogens are sp^2 hybridized. This is in contrast to the previously reported octahedral structure of $[NiL]^{2+}$, where three aniline pendant arms $R-NH_2$ are coordinated to nickel(II) and the nitrogens are sp^3 hybridized. It is interesting that the planes defined by the three-coordinate anilide nitrogens and the corresponding aromatic rings are nearly coplanar in all three cases in $[Mn(L\text{-}3H)]^+$; the dihedral angles between these planes are 12.2, 10.5, and 15.6°. Thus the three six-membered chelate rings are not quite equivalent in the solid state; the cation possesses only idealized C_3 symmetry. This inequivalency is nicely borne out in the infrared spectrum of $[Mn(L\text{-}3H)]BPh_4$ (KBr disk). In the region 3400−3200 cm^{-1} two sharp ν(N−H) stretching modes are observed at 3342 and 3314 cm^{-1} where the former shows a shoulder at ~3330 cm^{-1}. It is tempting to assign these three ν(N−H) frequencies with decreasing energy to the anilido groups with decreasing dihedral

---

(16) Koikawa, M.; Okawa, H.; Kida, S. *J. Chem. Soc., Dalton Trans.* **1988**, 641.

(17) Hockertz, J.; Steenken, S.; Wieghardt, K.; Hildebrandt, P. *J. Am. Chem. Soc.* **1993**, *115*, 11222.

(18) Hart, R. O. C.; Bott, S. G.; Atwood, J. L.; Cooper, S. R. *J. Chem. Soc., Chem. Commun.* **1992**, 894.

(19) Belal, A. A.; Chaudhuri, P.; Fallis, I.; Farrugia, L. J.; Hartung, R.; Macdonald, N. M.; Nuber, B.; Peacock, R. D.; Weiss, J.; Wieghardt, K. *Inorg. Chem.* **1991**, *30*, 4397.

(20) Pavacik, P. S.; Huffman, J. C.; Christou, G. *J. Chem. Soc., Chem. Commun.* **1986**, 43.

(21) Chandra, S. K.; Chakravorty, A. *Inorg. Chem.* **1992**, *31*, 760.

(22) Beissel, T.; Kesting, F.; Wieghardt, K. Unpublished results.

(23) Auerbach, U.; Weyhermüller, T.; Wieghardt, K.; Nuber, B.; Bill, E.; Butzlaff, C.; Trautwein, A. X. *Inorg. Chem.* **1993**, *32*, 508.

Table 6. Comparison of Mn−N and Mn−O Bond Distances in Mononuclear Octahedral Mn^{IV} Complexes

complex[a]	av Mn−N, Å	av Mn−O, Å	polyhedron	ref
$[Mn(HB(3,5\text{-}Me_2Pz)_3)_2](ClO_4)_2$	1.974		MnN_6	12
$[Mn(big)_3]OAc{\cdot}2H_2O$	1.934		MnN_6	18
$[Mn(L\text{-}3H)]BPh_4$	2.098 (amine) 1.877 (anilide)		MnN_6	this work
Mn TPP(NCO)$_2$	1.970 (porphyrine) 1.926 (NCO)		MnN_6	13
$[MnL']ClO_4$	2.046	1.839 (alkoxy)	MnN_3O_3	19
$[Mn(sal)_2(bipy)]$	2.048	1.829 (phenolate) 1.876 (carboxylate)	MnN_2O_4	20
$[Mn(saladhp)_2]$	2.005 (imine)	1.906 (phenolate) 1.854 (alkoxy)	MnN_2O_4	14
$[MnL^2]{\cdot}4H_2O$	2.038 (amine) 1.953 (amide)	1.848 (phenolate)	MnN_4O_2	21
$[MnL^3]{\cdot}MeOH$	2.084 (amine) 1.934 (amide)	1.858 (phenolate)	MnN_4O_2	21

[a] Ligand abbreviations: $\{HB(3,5\text{-}Me_2pz)_3\}^-$ = hydrotris(3,5-dimethylpyrazolyl)borate(1−); big$^-$ = biguanide(1−); TPP = tetraphenylporphinate(2−); L′ = 1,4,7-tris(2-hydroxyethyl)-1,4,7-triazacyclononanate(3−); sal = salicylate(2−): bipy = 2,2′-bipyridine; saladhp = 2-salicylideneaminato-1,3-dihydroxy-2-methylpropanate(2−); L^2 = 1,8-bis(2-hydroxybenzamido)-3,6-diazaoctanate(4−); L^3 = 1,10-bis(2-hydroxybenzamido)-4,7-diazadecanate(4−).

angles: the 3342 cm^{-1} (N−H) frequency corresponds to the anilido group with a dihedral angle of 15.5°, the ~3330 cm^{-1} frequency to the one with 12.2°, and the 3314 cm^{-1} mode to the one with 10.5°. With increasing dihedral angle, the N−H bond becomes stronger. It is significant that the $N_{anilide}-C_{phenyl}$ bond distances are rather short at an average value of 1.378 Å, which is to be compared with the $N_{aniline}-C_{phenyl}$ bond at 1.450 Å in $[NiL]^{2+}$.

Thus in $[Mn(L\text{-}3H)]^+$ this C−N bond has double-bond character whereas in $[NiL]^{2+}$ a C−N single bond prevails. The following resonance structure **C** depicts this situation:

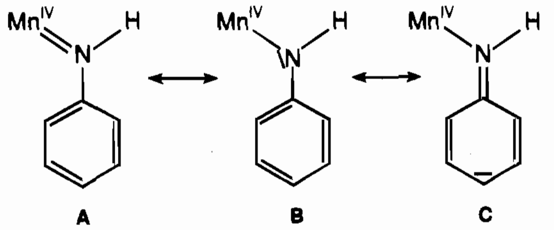

Since the ionic radius of an octahedral manganese(IV) ion is rather small (0.54 Å) and its charge high, this ion is expected to display a pronounced Lewis acidity toward an anilide anion. This is indeed the case. The average $Mn-N_{anilide}$ distance at 1.877 Å is the shortest Mn−N distance in octahedral manganese(IV) complexes observed to date and reflects the importance of resonance structure **A**. The compilation of structural data in Table 6 demonstrates this. The three facially bound anilido groups are good π-donors, and the $Mn-N_{anilide}$ bond has clearly double-bond character. Furthermore, these π-donors exert a structural trans influence on the $Mn-N_{amine}$ bonds in trans positions, which are comparatively long at 2.098 Å and, finally, the $N_{aniline}-Mn-N_{anilide}$ bond angles are slightly larger (average 93°) than the ideal octahedral angle of 90°.

Discussion

In this paper we have reported the electronic and geometric structures of a series of tri- or tetravalent octahedral first-row transition metal complexes which contain three facially bound anilido groups and three tertiary amine nitrogen donor atoms. The former are good σ- *and* π-donors whereas the latter must be considered pure σ-donors. Previously, we had synthesized a similar series of complexes containing in all cases a facially bound 1,4,7-triazacyclononane backbone (σ-donor) and, in addition, three facial alkoxo, phenolato, thiophenolato, or mercapto π-donor atoms. In all instances the octahedral high-spin d^5 iron(III) and the corresponding manganese(IV) and low-spin d^6 cobalt(III) species have been isolated and characterized. It is therefore possible to compare the structural and electronic properties of these different π-donors in a series of similar compounds. Chart 1 shows the complexes and gives their numbering scheme. We now wish to discuss their electronic spectral and structural properties summarized in Table 7.

Chart 1

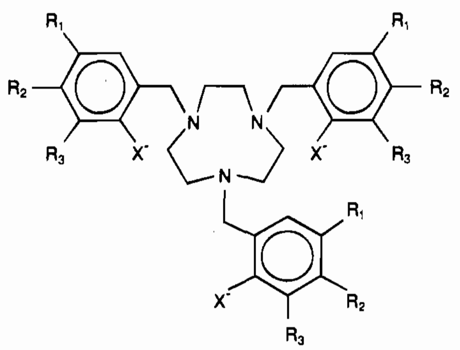

X	R_1	R_2	R_3	Complex	Ref.
O	$-C(CH_3)_3$	H	H	Mn^{IV} **1**, Fe^{III} **2**, Co^{III} **3**	23
O	H	H	H	Fe^{III} **4**	10
O	H	H	$-C(CH_3)_3$	Fe^{III} **5**, Co^{III} **6**	10
S	H	$-C(CH_3)_3$	H	Mn^{IV} **7**, Fe^{III} **8**, Co^{III} **9**	22, 8
NH	H	H	H	Mn^{IV} **10**, Fe^{III} **11**, Co^{III} **12**	this work

π-Donating properties can be structurally assessed by considering the influence of this donor on the bond length of the ligand in the trans position relative to it which in our cases is always an amine nitrogen π-donor. Thus, in the series $[Fe^{III}(tcta)]^{24}$ (tcta = 1,4,7-triazacyclononane 1,4,7-triacetate), **2**, and **5**, the iron is in a facial N_3O_3 donor set. The average Fe−N bond distnces are 2.181(3), 2.229(6), and 2.240(4) Å whereas the average Fe−O distances are 1.962(2), 1.918(6), and 1.889 Å, respectively. In [Fe(tcta)], all the donor atoms are to a first approximation σ-donors, in contrast to the phenolate oxygen donors in **2** and **5**, which are π-donors. Consequently, with

---

(24) Wieghardt, K.; Bossek, U.; Chaudhuri, P.; Herrmann, W.; Menke, B. C.; Weiss, J. *Inorg. Chem.* **1982**, *21*, 4308.

Table 7. Comparison of Electronic and Structural Data for Complexes of Mn^{IV}, Fe^{III}, and Co^{III} Containing a Facial N_3X_3 Donor Set

complex[a]	X → M charge transfer λ, nm (ϵ, L mol^{-1} cm^{-1})	av $M-N_{amine}$, Å	av M−X, Å	ref
1 ($Mn^{IV}O_3N_3$)	640 (7.07×10^3)			23
2 ($Fe^{III}O_3N_3$)	486 (4.86×10^3)	2.229(6)	1.918(6)	23
3 ($Co^{III}O_3N_3$)	562 (815), 377 (1.9×10^3)			23
4 ($Fe^{III}O_3N_3$)	459 (3.8×10^3)			10
5 ($Fe^{III}O_3N_3$)	479 (5.6×10^3)	2.240(4)	1.889(4)	10
6 ($Co^{III}O_3N_3$)	581 (490), 398 (sh)			10
7 ($Mn^{IV}S_3N_3$)	667 (5.5×10^3), ~700 (sh)			22
8 ($Fe^{III}S_3N_3$)	775 (4.52×10^3), 651 (6.11×10^3)	2.08(1)	2.280(6)	8
9 ($Co^{III}S_3N_3$)	652 (460), 523 (480)	2.04(3)	2.235(13)	22
10 ($Mn^{IV}N_3N_3$)	677 (4.0×10^3)	2.098(4)	1.877(4)	this work
11 ($Fe^{III}N_3N_3$)	587 (8.7×10^3)			this work
12 ($Co^{III}N_3N_3$)	600, 440			this work
[MnL′](ClO_4) ($Mn^{IV}O_3N_3$)	556 (750), 474 (850)	2.046(5)	1.839(4)	19

[a] For numbering scheme of complexes see Chart 1. $L'H_3$ = 1,4,7-tris(2-hydroxyethyl)-1,4,7-triazacyclononane.

increasing π-donor strength, the Fe−N bond distance in the trans position increases and the Fe−O bond distance decreases. Note that the sum of Fe−N and trans Fe−O distances is nearly invariant in the series at 4.14 ± 0.02 Å.

From a comparison of FeN_3O_3 complexes **2** and **5** with the FeN_3S_3 species **8**, it follows that a thiophenolate ligand is a weaker π-donor than a phenolate because the average $Fe-N_{amine}$ bond in **8** is much shorter than those in **2** and **5** and even shorter than that in [Fe(tcta)], which could be interpreted in the sense that thiophenolates have in fact π-acceptor properties. This bond length argument is not quite valid because **8** contains at room temperature a large amount of the low-spin form and the X-ray structure determination gives an average Fe−X value between those of the high- and low-spin forms.[8] Regrettably, we have not been able to grow single crystals of [Fe(L-3H)] in order to structurally assess the importance of π-donation of an anilide ligand in this series.

Comparison of the structure data for [MnL′](ClO_4)[19] (L′ = 1,4,7-tris(2-hydroxyethyl)-1,4,7-triazacyclononanate(3−)) and [Mn(L-3H)]BPh_4 reveals that the anilido groups exert a more effective trans influence on the $Mn-N_{amine}$ bond than the alkoxo ligands. As stated already above, the $Mn-N_{amine}$ bonds are the weakest and the $Mn-N_{anilide}$ bonds the strongest in $Mn^{IV}N_6$ complexes reported to date.

Solomon, Raymond, et al.[25] recently employed single-crystal polarized absorption and magnetic circular dichroism to elucidate the electronic structure of the iron(III) tris(catecholate) complex $[Fe(cat)_3]^{3-}$. The characteristic ligand-to-metal charge-transfer band in the visible region was found to be composed of two overlapping *x,y*-polarized transitions which are ligand π to metal d in nature. The energy difference between these transitions was found to be a direct measure for the amount of π bonding between the oxygen lone pairs and metal d orbitals (t_{2g} in O_h symmetry). By adapting their analysis for our idealized C_3-symmetric complexes with *fac*-N_3MX_3 polyhedra (X = phenolate, thiophenolate O or S donor, and anilide with an N donor), we arrive qualitatively at the following conclusions. (i) The high-spin iron(III) complexes and the manganese(IV) (d^3) species display a very intense ($\epsilon > 3.0 \times 10^3$ L mol^{-1} cm^{-1}) ligand-to-metal charge transfer (CT) band in the visible region which is absent in the spectra of the low-spin cobalt(III) (d^6) complexes. These observations corroborate the assignment as transition from ligand π to metal π^* orbitals (t_{2g} in O_h symmetry). (ii) The shape of these absorption maxima is in the phenolate and anilido complexes not symmetric and may well be composed of two overlapping Gaussian bands. It is interesting in this respect that, in the absorption spectra of the thiophenolate complexes **7** and **8**, *two* absorption maxima are in fact observed where the energy differences are 706 and 2458 cm^{-1}, respectively. For tris(catecholato)iron(III) complexes, this difference is larger at 3500−4300 cm^{-1}. (iii) The spectrum of the tris(acetato) complex [Fe(tcta)] is featureless in the visible region and thus corroborates our above notion that the coordinated carboxylate oxygen atoms are pure σ-donors. It is also noteworthy that the trialkoxy complex [MnL′](ClO_4) displays two bands of relatively low intensity in the visible region. These bands may be d−d transitions rather than ligand-to-metal CT transitions. This implies that in this case the alkoxy ligands are rather poor π-donors in contrast to the phenolate ligands in **1**.

In summary, structural and electronic spectral data of the series of iron(III) complexes **2**, **4**, **5**, **8**, and **11** confirm that phenolates and anilides are strong π-donors whereas this property is much less pronounced for thiophenolates. The same conclusion is drawn from the data for manganese(IV) complexes **1**, **7**, and **10** although the difference between thiophenolates, on one hand, and anilide and phenolates, on the other hand, is probably less developed.

Acknowledgment. We thank the Fonds der Chemischen Industrie for financial support of this work. Dr. H. Grondey (University of British Columbia, Vancouver) is thanked for measuring the solid state ^{13}C NMR spectrum and Dr. E. Bill (Medizinische Universität Lübeck) for recording the ESR spectrum.

Supporting Information Available: Listings of bond lengths and angles, hydrogen atom coordinates, anisotropic thermal parameters, and full details of intensity collection and refinement (9 pages). Ordering information is given on any current masthead page.

IC9507169

---

(25) Karpishin, T. B.; Gebhard, M. S.; Solomon, E. I.; Raymond, K. N. *J. Am. Chem. Soc.* **1991**, *113*, 2977.